Identification of Switching Mechanism in Molecular Junctions by Inelastic Electron Tunneling Spectroscopy

Hui Cao,[†,‡] Jun Jiang,[†] Jing Ma,[‡] and Yi Luo*[,†]

Department of Theoretical Chemistry, School of Biotechnology, Royal Institute of Technology, S-106 91 Stockholm, Sweden, and School of Chemistry and Chemical Engineering, Institute of Theoretical and Computational Chemistry, Key Laboratory of Mesoscopic Chemistry of MOE, Nanjing University, Nanjing 210093, China

Received: January 30, 2008; Revised Manuscript Received: May 6, 2008

We present first-principles studies on electron transport properties of Pd-dithiolated oligoaniline−Pd molecular junctions. It is to demonstrate the possibility of using inelastic electron tunneling spectroscopy (IETS) to identify the switching mechanism in the molecular junction. Calculations have successfully reproduced the experimentally observed conductance switching behavior and the corresponding inelastic electron tunneling spectra. It is shown that the conductance switching is induced by conformation changes of the intercalated dithiolated oligoaniline in the junctions rather than oxidation/reduction as proposed earlier. Among three possible isomers, the low and high conductance states are related to two symmetrical structures. The possible involvement of asymmetric structure is discussed. It is revealed that chemical bonds between the terminal S atom and Pd electrodes are quite weak with relatively long bond distances.

The conductance switching of two-terminal molecular junctions has attracted much attention[1–4] owing to its importance for molecular electronic devices. Various possible mechanisms for such switching behavior have been proposed, including oxidation/reduction of molecules,[1,5,6] rotation of functional groups,[7] rotation of molecular backbones,[8] interactions with neighbor molecules,[9] fluctuation of bonds,[10–12] and change of molecule−metal hybridization.[13,14] However, the lack of a proper characterization tool to determine the exact structure of the molecule in the junction has made it difficult to distinguish different mechanisms. In this context, inelastic electron tunneling spectroscopy (IETS) has proven to be very useful.[15–22] In the electronic off-resonant region, peaks in IETS correspond to frequencies of the excited vibrational normal modes of intercalated molecules. With the help of theoretical simulations, one can identify not only the conformation changes of the molecule in the junctions[17,19] but also the exact bonding distance between the terminal atoms in the molecule and the electrodes.[22]

Recently, Cai et al.[23] observed a switching behavior between two bistable conductance states in the in-wire junctions of dithiolated *N*-methyl-oligoaniline dimer. For this bistable switching, a possible mechanism related to the charging effect had been proposed,[23] which was later challenged by a theoretical study of Sotelo et al.[24] who have calculated elastic current−voltage characteristics of the molecular junctions and found that the conductance switching can be explained by the change of molecular confirmation between two stable conjugated structures of the oligoaniline dimer. However, their calculations cannot rule out the charging mechanism, and the calculated ratio between high and low conductance states is much smaller than that of the experiment. To resolve this conflict or other controversies in this field, one has to go beyond elastic electron tunneling. Fortunately, Cai et al.[23] have also measured the IETS spectra of high and low conductance states. One can thus hope that a comparison between theoretical and experimental IETS spectra should lead to a definitive conclusion on the switching mechanism.

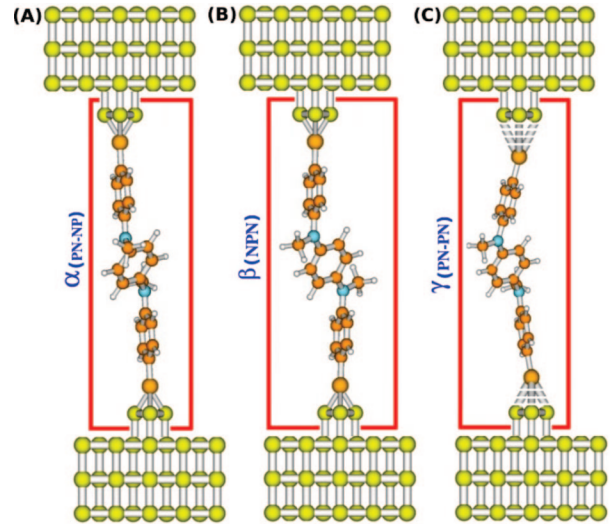

Figure 1. Structures of Pd-dithiolated oligoaniline dimer−Pd junctions with three different conjugated structures: (A) $\alpha_{(PN\text{-}NP)}$ (both N-CH_3 bonds are coplanar with the outer phenyl rings), (B) $\beta_{(NPN)}$ (both N-CH_3 bonds are coplanar with the inner phenyl ring), and (C) $\gamma_{(PN\text{-}PN)}$ (one N-CH_3 bond is coplanar with the outer phenyl ring and another is coplanar with the inner phenyl ring).

In the present work, we report the first-principles simulations for IETS spectra of dithiolated oligoaniline dimer intercalated between two Pd contacts. It is noted, as also pointed out by Sotelo et al.,[24] that the oligoaniline dimer has three different isomers with distinct conjugations, whose structures are illustrated in Figure 1. Following the terminology of Sotelo et al.,[24] we have also named the three isomers as $\alpha_{(PN\text{-}NP)}$, $\beta_{(NPN)}$, and $\gamma_{(PN\text{-}PN)}$ conjugations. In the case of $\alpha_{(PN\text{-}NP)}$ conjugation,

* To whom correspondence should be addressed. E-mail: luo@theochem.kth.se.
† Royal Institute of Technology.
‡ Nanjing University.

10.1021/jp800884g CCC: $40.75
Published on Web 06/27/2008

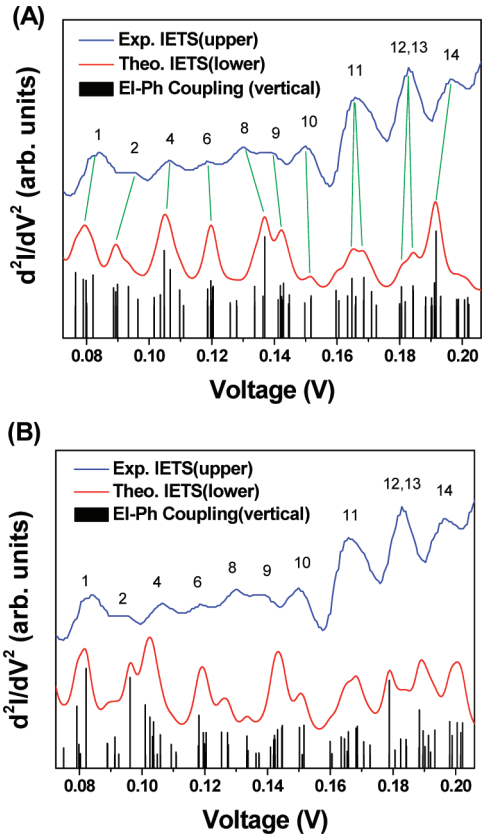

Figure 2. Calculated IETS spectra for molecular junctions of (A) $\alpha_{(PN-NP)}$ conjugation and (B) $\gamma_{(PN-PN)}$ conjugation (lower curves in red) together with the experimental IETS spectrum of the low conductance state[20] (upper curves in blue). The gap distance between two Pd electrodes is 19.90 Å, and the working temperature is 10 K. IETS strengths of individual vibrational modes for both conjugations are given as black vertical lines.

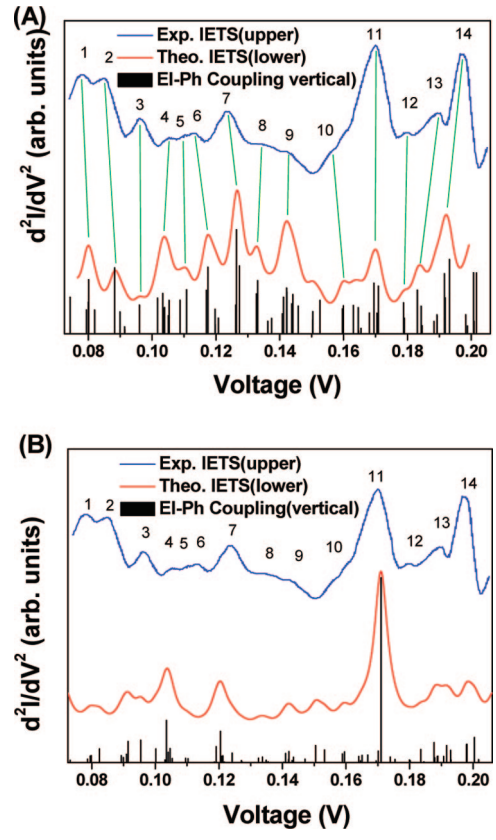

Figure 3. Calculated IETS spectra for molecular junctions of (A) $\beta_{(NPN)}$ conjugation and (B) a positively charged molecule (lower curves in red) together with the experimental IETS spectrum of the high conductance state[20] (upper curves in blue). The gap distance between two Pd electrodes is 19.90 Å, and the working temperature is 10 K. IETS strengths of individual vibrational modes for both conjugations are given as black vertical lines.

both N-CH_3 bonds are coplanar with the outer phenyl rings. When this bond becomes coplanar with the inner phenyl ring, we have the $\beta_{(NPN)}$ conjugation. Both $\alpha_{(PN-NP)}$ and $\beta_{(NPN)}$ conjugations are of symmetric structure. The third conjugation, $\gamma_{(PN-PN)}$, has an asymmetric structure, in which one of the N-CH_3 bonds is coplanar with the outer phenyl ring while another is coplanar with the inner phenyl ring. Both elastic and inelastic electron tunneling properties for all three conjugations have been calculated using our recently developed generalized quantum chemical approach[19] implemented in the QCME program.[25] It is noted that a harmonic approximation is adopted in our method and the heating effect caused by vibronic excitations is not taken into account. Geometries and electronic structures of isolated diothiolated oligoaniline dimer in the gas phase have been optimized using the Gaussian03 program package[26] at the hybrid B3LYP functional[27,28] level with the 6-31G(d) basis set and the LanL2DZ[29] pseudo potential basis set being applied to nonmetal elements and Pd, respectively. Upon adsorption, both terminal S atoms form direct chemical bonds with the Pd electrodes. It is assumed that the S atoms are placed on the top of the center of three Pd atoms in a Pd (111) plane. The potential energy surface of the extended $\alpha_{(PN-NP)}$ conjugation system with respect to the distance between two electrodes is obtained for the molecule, and two local minima at distances of 18.48 and 19.90 Å, respectively, have been identified. It is found that for such extended systems the unrestricted density functional method needs to be used to calculate their electronic structures.

Calculations show that the $\alpha_{(PN-NP)}$ conjugation has the lowest energy (−1680.0324796 au) among the three isomers, while the $\gamma_{(PN-PN)}$ and $\beta_{(NPN)}$ conjugations are about 0.01 and 0.08 eV higher in energy, respectively. From an energetic point of view, both $\alpha_{(PN-NP)}$ and $\gamma_{(PN-PN)}$ structures can be considered as the low conductance state, while $\beta_{(NPN)}$ conjugation is the high conductance state. Our calculated zero-bias conductances have values of 0.51 μS (0.0066G_0), 0.95 μS (0.012G_0), and 9.78 μS (0.12G_0) for the $\alpha_{(PN-NP)}$, $\gamma_{(PN-PN)}$, and $\beta_{(NPN)}$ junctions, respectively. The order of zero-bias conductance is thus exactly the same as the order of the energy. It is noted that the ratio between the zero-bias conductance of $\alpha_{(PN-NP)}$ and $\gamma_{(PN-PN)}$ conjugations is less than 2, consistent with the result of Sotelo et al.[24] Our calculated zero-bias conductance ratio between $\beta_{(NPN)}$ and $\alpha_{(PN-NP)}$ conjugations is 19, which is in good agreement with the experiments[23] but differs greatly from the calculations of Sotelo et al.[24] whose value is less than 2. It can thus be concluded that the high conductance state found in the experiment should be of $\beta_{(NPN)}$ conjugation rather than the $\gamma_{(PN-PN)}$ conjugation as suggested by Sotelo et al.[24] To further confirm our assignment, we have carried out IETS calculations for molecular junctions with three different conjugations.

Our calculations have found that the calculated IETS spectra for $\alpha_{(PN-NP)}$ and $\beta_{(NPN)}$ conjugations are indeed in good agreement with the experimental spectra of low and high conductance states, respectively. It is noted that a common line width of 4 meV is adopted for all spectral lines in order to directly compare with the experiments. Figure 2A presents the calculated IETS spectrum for the junction of $\alpha_{(PN-NP)}$ conjugation with an electrode gap distance of 19.90 Å, together with the experimental spectrum of the low conductance state[23] at a temperature of 10

TABLE 1: Assignments for Vibrational Modes in IETS Spectra of Low and High Conductance States in the Pd-Dithiolated Oligoaniline Dimer−Pd Junctions

		peak (mV)						
		low state			high state			
	mode	exp[a]	calc	Δ[b]	exp[a]	calc	Δ[b]	shift[c]
1	δ_s(C═C in phenyl rings)	82.7	78.9	−3.8	77.8	80.1	2.3	1.2
2	γ_t(outer phenyl ring)	95.7	89.9	−5.8	85.3	88.3	3.0	−1.6
3	mixed δ_s(C═C in phenyl rings) and ν(N−C (in CH3))				96.1	96.3	0.2	
4	γ_w(C−H in phenyl rings)	106.1	104.8	−1.3	104.8	103.9	−0.9	−0.9
5	mixed δ_s(C═C in phenyl rings) and $\gamma_w(CH_3)$				109.7	110.8	1.1	
6	γ_w(C−H in phenyl rings)	118.2	119.7	1.5	113.3	117.2	3.9	−2.5
7	δ_s(C═C in phenyl rings)				123.4	126.6	3.2	
8	δ_s(C−H in phenyl rings)	129.6	136.9	7.3	134.5	133.1	−1.4	−3.7
9	mixed $\gamma_w(CH_3)$ and δ_s(C−H in phenyl rings)	139.7	142.4	2.7	143.3	142.2	−1.1	−0.2
10	δ_s(C−H in phenyl rings)	150.1	151.7	1.6	155.1	159.8	4.7	8.1
11	δ_s(C−H in phenyl rings)	165.8	165.9	0.1	170.1	169.8	−0.3	3.9
	ν(aromatic C−N)	165.8	168.5	2.7	170.1	169.8	−0.3	1.3
12	ν(C═C in phenyl rings)	182.8	180.5	−2.3	179.5	179.0	−0.5	−1.5
13	$\gamma_w(CH_3)$	182.8	184.4	1.6	189.6	184.3	−5.3	−0.1
14	mixed $\gamma_w(CH_3)$ and δ_s(C−H in phenyl rings)	196.1	191.1	−5.0	196.8	191.7	−5.1	0.6

[a] Reference 20. [b] Difference between experimental and calculated results. [c] Calculated energy shift between the same vibrational mode in the low and high current states.

K for comparison. It can be seen that all experimental spectral features, as well as overall spectral intensity distribution, are closely reproduced by the calculations. With the same electrode structures, we have also calculated the IETS spectrum of another low conductance state, $\gamma_{(PN\text{-}PN)}$, shown in Figure 2B. In comparison with that of $\alpha_{(PN\text{-}NP)}$ conjugation, more spectral features can be found in the spectrum of $\gamma_{(PN\text{-}PN)}$ conjugation due to its lower symmetry. It is noted that, in the high energy region (above 0.16 V), the spectrum has quite poor agreement with the experiment. It is also noted that in the gas phase the $\gamma_{(PN\text{-}PN)}$ conjugation is only 0.01 eV higher than the $\alpha_{(PN\text{-}NP)}$ conjugation in energy. Although at the experimental working temperature of 10 K the population of $\gamma_{(PN\text{-}PN)}$ conjugation is very small according to the Boltzmann distribution at the zero-bias, one might argue that under the external bias its presence might increase considerably. We have tested to mix the spectra of $\alpha_{(PN\text{-}NP)}$ and $\gamma_{(PN\text{-}PN)}$ conjugations with different proportions but failed to improve the agreement between theoretical and experimental spectra. It might due to the high energy barrier for conformation change from $\alpha_{(PN\text{-}NP)}$ conjugation to $\gamma_{(PN\text{-}PN)}$ conjugation[24] that has prevented the presence of $\gamma_{(PN\text{-}PN)}$ conjugation.

The calculated IETS spectrum of $\beta_{(NPN)}$ conjugation resembles the experimental spectrum of the high conductance state very well, as nicely demonstrated in Figure 3A. We have also calculated the IETS spectrum of the positively charged (+1) molecule of $\alpha_{(PN\text{-}NP)}$ conjugation to examine the possible oxidation effect. The calculated spectrum for the oxidation state differs significantly from that of the experimental spectrum of the high current state. As can be seen in Figure 3B, several major spectral features, such as peaks 1 and 2, peaks 4−6, and peaks 12 and 13, all disappear in the calculated one. It seems that the charging of the molecule has localized the IETS spectrum to a particular vibration mode. This behavior seems to be quite similar to what has been found in the IETS spectrum of the Gd@C_{82} molecule adsorbed on a metal surface.[30] Furthermore, the calculated oxidation energy for the oligoaniline dimer is around 5.7 eV, much higher than the external voltage of 3.5 V needed for the conductance switching.[23] Our calculations for the total energy, zero-bias conductance and more importantly IETS thus favor a switching mechanism related to the conjugation changes rather than the charging effect.

The good agreement between theory and experiment allows us to assign the experimental IETS spectra in detail. The characters of vibrational modes that have been observed in the experimental IETS spectra of both low and high current states are described in Table 1. Because our simulated IETS spectra are based on calculation of the coupling strength between electrons and phonons, our assignment should be more relevant than those made from IR and Raman spectra of the isolated molecule.[20] For example, the peak at 196.1 mV in the spectrum of the low current state is found to be the mixed mode of wagging $\gamma_w(CH_3)$ and scissoring δ_s(C−H in phenyl rings) and not a pure C═C stretching mode as assigned in ref 20. A few interesting things are worth mentioning here. In general, the scissoring modes of phenyl rings, such as δ_s(C═C) and δ_s(C−H), have high intensity. We have also found that peaks labeled as 3, 5, and 7 in the spectrum of the high current state do not have their counterparts in the low current state spectrum. All these three vibration modes are related to the δ_s(C═C in phenyl rings) mode. In the high current state, that is, $\beta_{(NPN)}$ conjugation, the C═C scissoring modes of phenyl rings have larger components along the direction of electron transport, making them more active according to the basic IETS selection rule. Moreover, we have found that the experimental peak at 182.8 mV of the low current state IETS spectrum is composed of two different modes, namely, the stretching mode of ν(C═C in phenyl rings) and the wagging mode of $\gamma_w(CH_3)$. In the high current state IETS spectrum, these two peaks become nondegenerated. The cause of the separation is due to the conjugation change from $\alpha_{(PN\text{-}NP)}$ to $\beta_{(NPN)}$ which is accompanied by the rotation of the CH_3 group.

We have shown in our previous studies that IETS not only distinguishes the conformation changes in the molecular junction[18] but also determines the bond distance between the molecule and the electrodes.[22] It was mentioned that at the Pd−Pd electrode distance of 18.48 Å, another energy minimum was found in the $\alpha_{(PN\text{-}NP)}$ conjugation molecular junction. Energetically, it is more stable than that at a distance of 19.90 Å. However, the energy profile was computed for an extended molecule with two three-Pd-atom clusters connected to each end of the molecule. The calculated equilibrium distance might not correspond to the experimental conditions. We have instead used the IETS spectra to verify it. The calculated IETS spectra

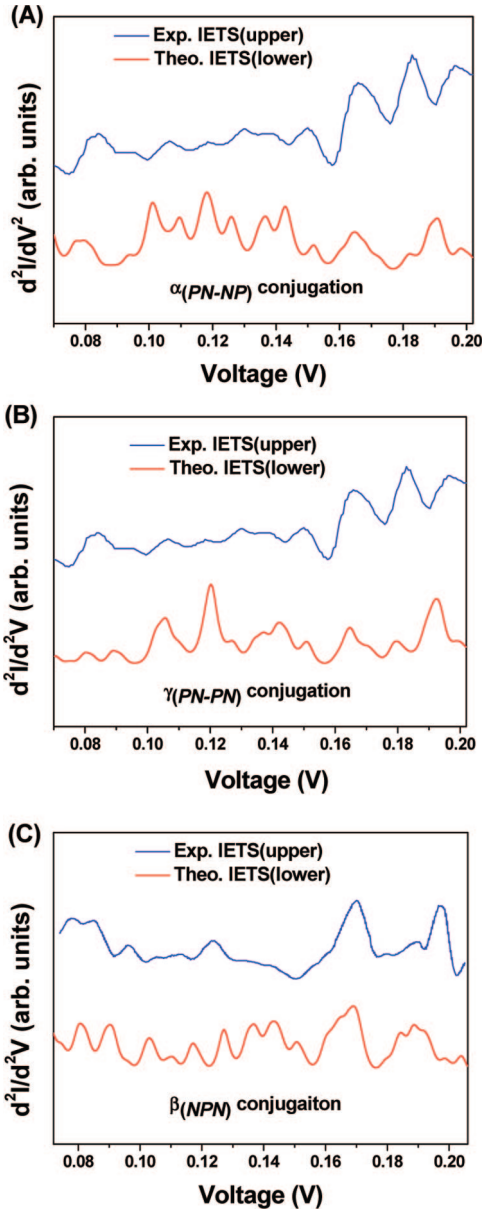

Figure 4. Calculated IETS spectra for (A) $\alpha_{(PN\text{-}NP)}$, (B) $\gamma_{(PN\text{-}PN)}$, and (C) $\beta_{(NPN)}$ conjugations (lower curves in red), together with experimental IETS[20] spectra of the low conductance state (upper curve in blue in (A) and (B)) and high conductance state (upper curve in blue in (C)). The gap distance between two Pd electrodes is 18.48 Å, and the working temperature is 10 K.

for molecular junctions of $\alpha_{(PN\text{-}NP)}$, $\beta_{(NPN)}$, and $\gamma_{(PN\text{-}PN)}$ conjugations with an electrode gap distance of 18.48 Å are shown in Figure 4. It can be seen in Figure 4A that the agreement between the calculated IETS spectrum of $\alpha_{(PN\text{-}NP)}$ conjugation and the experimental spectrum of the low conductance state becomes poorer. By shortening the bond distance of S−Pd, more vibrational modes are active and the spectral intensities at the high energy region (160−200 mV) are significantly reduced. The calculated IETS spectrum of $\gamma_{(PN\text{-}PN)}$ conjugation is given in Figure 4B and does not show any improved agreement with the experiment. It is interesting to see that, at this bond distance, the IETS spectrum of $\alpha_{(PN\text{-}NP)}$ conjugation consists of as many structures as $\gamma_{(PN\text{-}PN)}$ conjugation, despite the fact that $\alpha_{(PN\text{-}NP)}$ conjugation has a relatively high symmetry. Such a bond length dependent behavior highlights the difficulty of finding the general selection rules for IETS, which is too much dependent on the actual geometry of the molecule inside the junction. The

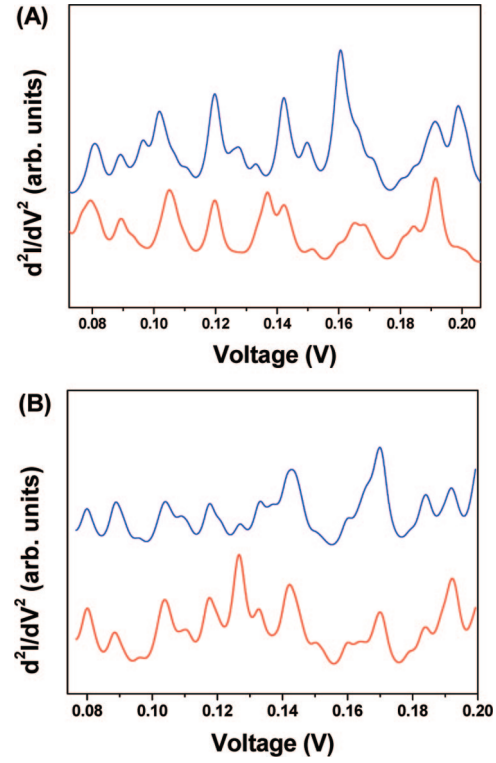

Figure 5. Comparison of IETS spectra between two bonding configurations for the (A) low conductance state and (B) high conductance state. The upper curves are IETS spectra from the extended molecule Pd_4-M-Pd_4, while the lower ones are from Pd_3-M-Pd_3.

IETS spectrum of $\beta_{(NPN)}$ conjugation is given in Figure 4C. Similar to the cases of the $\alpha_{(PN\text{-}NP)}$ and $\gamma_{(PN\text{-}PN)}$ conjugations, the reduction of bond length has activated more vibration modes, resulting in a broader spectral profile. Nevertheless, the agreement between theory and experiment at this bond length is considerably poor. Based on the IETS calculations, we can thus conclude that the molecule is loosely bonded to the metal electrodes.

It was shown in the work of Ke et al.,[31] the change of the bonding configuration at the molecule−electrode interface can strongly affect the transport behavior of the molecular junctions. It is thus interesting to see how sensitive the IETS spectra are to the interfacial bonding configurations. We have adopted a model, similar to what was suggested by Ke et al.,[31] by putting one additional Pd atom on top of each triangle Pd cluster, which is directly connected to the molecule. The structure is named as Pd_4-M-Pd_4. A comparison between IETS spectra of the two different bonding configurations for both the low and high conductance states is shown in Figure 5. One can find that the characteristic peaks, especially between 120 and 140 mV, are quite different between the two cases. It has further confirmed that IETS spectra are indeed sensitive to the change of the bonding configurations at the molecule−electrode interface as observed in our previous study.[22]

In summary, we have carried out hybrid density functional theory calculations for IETS spectra of oligoaniline dimer dithiolates chemically bonded between two Pd electrodes. Effects of conjugation changes and oxidation on IETS spectra have been discussed and compared with the experimental spectra. It is shown that the experimentally observed conductance switching is most likely to be induced by the conjugation change rather than the charging. Such a conclusion is also supported by comparing the total energy and zero-bias conductance of different conjugated structures. This study demonstrates

yet again the power of IETS for identifying the structure of a molecule in a molecular junction.

Acknowledgment. This work was supported by the Swedish Research Council (VR), the Swedish Infrastructure for Computing (SNIC), and the Nature Science Foundation of China (No. 20573050).

References and Notes

(1) Chen, J.; Reed, M. A.; Rawlett, A. M.; Tour, J. M. *Science* **1999**, *286*, 1550.
(2) Donhauser, Z. J.; Mantooth, B. A.; Kelly, K. F.; Bumm, L. A.; Monnell, J. D.; Stapleton, J. J.; Price, D. W.; Rawlett, A. M.; Allara, D. L.; Tour, J. M.; Weiss, P. S. *Science* **2001**, *292*, 2303.
(3) Blum, A. S.; Kushmerick, J. G.; Long, D. P.; Patterson, C. H.; Yang, J. C.; Henderson, J. C.; Yao, Y. X.; Tour, J. M.; Shashidhar, R.; Ratna, B. R. *Nat. Mater.* **2005**, *4*, 167.
(4) Gaudioso, J.; Lauhon, L. J.; Ho, W. *Phys. Rev. Lett.* **2000**, *85*, 1918.
(5) Seminario, J. M.; Zacarias, A. G.; Tour, J. M. *J. Am. Chem. Soc.* **2000**, *122*, 3015.
(6) Seminario, J. M.; Zacarias, A. G.; Derosa, P. A. *J. Phys. Chem. A* **2001**, *105*, 791.
(7) Di Ventra, M.; Kim, S. G.; Pantelides, S. T.; Lang, N. D. *Phys. Rev. Lett.* **2001**, *86*, 288.
(8) Cornil, J.; Karzazi, Y.; Brédas, J. L. *J. Am. Chem. Soc.* **2002**, *124*, 3516.
(9) Lang, N. D.; Avouris, P. *Phys. Rev. B* **2000**, *62*, 7325.
(10) Ramachandran, G. K.; Hopson, T. J.; Rawlett, A. M.; Nagahara, L. A.; Primak, A.; Lindsay, S. M. *Science* **2003**, *300*, 1413.
(11) Keane, Z. K.; Ciszek, J. W.; Tour, J. M.; Natelson, D. *Nano Lett.* **2006**, *6*, 1518.
(12) Danilov, A. V.; Kubatkin, S. E.; Kafanov, S. G.; Flensberg, K.; Bjørnholm, T. *Nano Lett.* **2006**, *6*, 2184.
(13) He, J.; Fu, Q.; Lindsay, S.; Ciszek, J. W.; Tour, J. M. *J. Am. Chem. Soc.* **2006**, *128*, 14828.
(14) Moore, A. M.; Dameron, A. A.; Mantooth, B. A.; Smith, R. K.; Fuchs, D. J.; Ciszek, J. W.; Maya, F.; Yao, Y.; Tour, J. M.; Weiss, P. S. *J. Am. Chem. Soc.* **2006**, *128*, 1959.
(15) Kushmerick, J. G.; Lazorcik, J.; Patterson, C. H.; Shashidhar, R.; Seferos, D. S.; Bazan, G. C. *Nano Lett.* **2004**, *4*, 639.
(16) Wang, W. Y.; Lee, T.; Kretzschmar, I.; Reed, M. A. *Nano Lett.* **2004**, *4*, 643.
(17) Troisi, A.; Ratner, M. A. *Phys. Rev. B* **2005**, *72*, 033408.
(18) Jiang, J.; Kula, M.; Lu, W.; Luo, Y. *Nano Lett.* **2005**, *5*, 1551.
(19) Jiang, J.; Kula, M.; Luo, Y. *J. Chem. Phys.* **2006**, *124*, 034708.
(20) Paulsson, M.; Frederiksen, T.; Brandbyge, M. *Nano Lett.* **2006**, *6*, 258.
(21) Long, D. P.; Lazorcik, J. L.; Mantooth, B. A.; Moore, M. H.; Ratner, M. A.; Troisi, A.; Yao, Y.; Ciszed, J. W.; Tour, J. M.; Shashidhar, R. *Nat. Mater.* **2006**, *5*, 901.
(22) Kula, M.; Jiang, J.; Luo, Y. *Nano Lett.* **2006**, *6*, 1693.
(23) Cai, L.; Cabassi, M. A.; Yoon, H.; Cabarcos, O. M.; McGuiness, C. L.; Flatt, A. K.; Allara, D. L.; Tour, J. M.; Mayer, T. S. *Nano Lett.* **2005**, *5*, 2365.
(24) Sotelo, J. C.; Yan, L.; Wang, M.; Seminario, J. M. *Phys. Rev. A* **2007**, *75*, 022511.
(25) Jiang, J.; Luo, Y. *QCME-V1.0: Qunatum Chemistry for Molecular Electronics*; Royal Institute of Technology: Stockholm, Sweden, 2005.
(26) Frisch, M. J.; *Gaussian03*, revision A.1; Gaussian, Inc.: Wallingford, CT, 2004.
(27) Becke, A. D. *J. Chem. Phys.* **1993**, *98*, 5648.
(28) Lee, C.; Yang, W.; Parr, R. G. *Phys. Rev. B* **1988**, *37*, 785.
(29) Hay, P. J.; Wadt, W. R. *J. Chem. Phys.* **1985**, *82*, 270.
(30) Grobis, M.; Khoo, K. H.; Yamachika, R.; Lu, X.; Nagaoka, K.; Louie, S. G.; Crommie, M. F.; Kato, H.; Shinohara, H. *Phys. Rev. Lett.* **2005**, *94*, 136802.
(31) Ke, S.-H.; Baranger, H. U.; Yang, W. T. *J. Chem. Phys.* **2005**, *122*, 074704.

JP800884G